K^+ channel regulation of signal propagation in dendrites of hippocampal pyramidal neurons

Dax A. Hoffman, Jeffrey C. Magee*, Costa M. Colbert & Daniel Johnston

Division of Neuroscience, Baylor College of Medicine, Houston, Texas 77030, USA

Pyramidal neurons receive tens of thousands of synaptic inputs on their dendrites. The dendrites dynamically alter the strengths of these synapses and coordinate them to produce an output in ways that are not well understood. Surprisingly, there turns out to be a very high density of transient A-type potassium ion channels in dendrites of hippocampal CA1 pyramidal neurons. These channels prevent initiation of an action potential in the dendrites, limit the back-propagation of action potentials into the dendrites, and reduce excitatory synaptic events. The channels act to prevent large, rapid dendritic depolarizations, thereby regulating orthograde and retrograde propagation of dendritic potentials.

Neuronal dendrites contain a variety of voltage-gated Na^+ and Ca^{2+} channels that enable action potentials and excitatory postsynaptic potentials (EPSPs) to propagate actively throughout the neuron (reviewed in refs 1, 2). Although our understanding of information processing in neurons is increasing, several fundamental aspects of dendritic physiology remain unexplained. Until now, reports of dendritic action-potential threshold and amplitude, as well as the small, active EPSP component, have suggested that the dendritic membrane is weakly excitable compared with the somatic membrane[3–11], which is inconsistent with the comparable density of Na^+ and Ca^{2+} channels in these two regions[3–5].

Our elementary knowledge about dendritic K^+ channels[10,12] means that our understanding of dendritic electrical properties is incomplete. We show here that the dendrites of CA1 pyramidal neurons have a high density of transient A-type K^+ channels and that this density increases with distance from the soma. The presence of these dendritic channels causes action-potential amplitude to decrease with distance from the soma, inhibits the ability of dendrites to initiate action potentials, and alters the shape of EPSPs. Furthermore, several key voltage-dependent properties of these channels allow for the unique regulation of dendritic excitability by subthreshold synaptic activity. Such a feature could be important for the induction of associative synaptic plasticity[13–15]. By severely dampening dendritic excitability, A-type K^+ channels play the dominant role in determining the electrical properties of CA1 dendrites and thereby influence dendritic integration and propagation of information.

Dendritic density of transient K^+ channels

To characterize the properties and distribution of K^+ channels in a central neuron, we have used cell-attached patch-clamp recordings from the soma and apical dendrites of CA1 hippocampal pyramidal neurons. These recordings revealed a high density of outward current composed of two distinct components separated through the use of standard subtraction procedures[16]. The first component was a transient component that rapidly activated and inactivated; the second component was more slowly inactivating. The recorded density of the transient component increased linearly with distance from the soma (slope, 12.5 pA per 100 μm) (Fig. 1a). The peak current density of transient channels increased from an average of 8.32 ± 1.38 pA per patch (mean ± s.e.m.) in the soma to 51.56 ± 9.47 pA in the distal dendrites for a voltage step from -85 to 55 mV. The current density of the sustained, non-inactivating component remained constant, with an average of 8.39 ± 1.46 pA per patch in the soma and 9.55 ± 1.84 pA per patch in the distal dendrites. Representative traces from the soma and distal dendrite of both the transient and sustained component are shown in Fig. 1b. Single channel recordings such as those in Fig. 1c were used to construct the I–V curve in Fig. 1d. A linear-regression fit of the data reveals that the transient component comprises small conductance (~7.5 pS) channels whose unitary current amplitude reverses near the K^+ equilibrium potential.

Steady-state activation and inactivation curves were generated for both the transient and sustained components (Fig. 2a,b). These curves reveal that the transient component activates at slightly more hyperpolarized potentials than the sustained component, and that significant transient-channel activation will occur at relatively hyperpolarized potentials (compare Fig. 2a,b). This particularly applies to transient channels located in the distal dendrites, which had an activation curve that was shifted 12 mV hyperpolarized compared to that from the soma/proximal (up to 100 μm) dendrites (Fig. 2a). The time course of activation was rapid (~1 ms) and was relatively constant over the range of voltages tested. The steady-state inactivation curves for the transient component did not vary with distance from the soma (Fig. 2a), and the sustained component had a steady-state activation curve that was also independent of patch location (Fig. 2b). The time constant of inactivation for the transient component increased linearly with amount of depolarization from 6.1 ± 0.4 ms for a step to -25 mV up to 27.3 ± 1.9 ms for a step to +55 mV (Fig. 2c). Similar results were obtained using outside-out patches ($n = 3$, data not shown). Thus, both an increased transient current density and a more hyperpolarized activation range should increase the impact of these channels on more distal dendrites.

4-Aminopyridine (4-AP), tetraethylammonium (TEA), and α-dendrotoxin (DTX) were applied to outside-out patches pulled from the soma and dendrites. In no case did the location from which the patch was taken have a discernible effect on drug efficacy. 4-AP reduced the transient component in a dose-dependent manner while having only a slight antagonist effect on the sustained component (Fig. 2d). TEA reduced both components similarly at

* Present address: Neuroscience Center, Louisiana State University Medical Center, New Orleans, Louisiana 70112, USA.

0.1 and 1.0 mM but had a larger effect on the sustained component at 10 mM (Fig. 2e). DTX has been reported to preferentially reduce a transient K^+ conductance with kinetics and 4-AP sensitivities separate from the transient A-type channels[17–19]. DTX (1 μM) reduced the transient component by 21.83 ± 6.67% ($n = 6$; data not shown).

The voltage-activated outward current described above appears to be composed of at least three components. The primary component is a large, transient, DTX-insensitive current that possesses voltage-dependent and pharmacological properties most similar to those generally ascribed to A-type K^+ channels[16–22]. A small fraction of the transient current was DTX-sensitive, which may indicate a second channel type. Finally, the sustained component demonstrated voltage-dependent and pharmacological properties similar to delayed-rectifier-type K^+ channels. The elevated density of dendritic A-type channels reported here agrees with immunohistochemistry studies that found an increased density of the transient K^+ channel subtype Kv 4.2 in the distal dendrites of CA1 pyramidal neurons[23,24]. Another recent study has found Kv 4.2 clustered on the postsynaptic membrane directly apposed to the presynaptic terminal[25].

Role of A-channels

A large outward conductance that both activates and inactivates very rapidly over relatively hyperpolarized voltage ranges could potentially have a profound impact on the electrical properties of dendrites. Such a conductance would act like a shock absorber to limit large, rapid dendritic depolarizations. CA1 and neocortical pyramidal cell types contain voltage-gated Na^+ and Ca^{2+} channel densities that are uniform for what appears to be the entire extent of the somatodendritic axis[3,5]. The increasing density of dendritic A-channels could explain why, in the face of this uniform inward conductance, the amplitude of back-propagating action potentials decreases with distance from the soma, why action potentials initiate in the axonal–somatic region as opposed to the dendrites, and why dendritic Na^+ and Ca^{2+} channels seem to have only a slight impact on subthreshold EPSPs. To assess the functional impact of the increasing density of A-type channels in the dendrites, simultaneous dendritic and somatic whole-cell voltage recordings were made from CA1 pyramidal neurons in hippocampal slices. Blockade of mainly A-type K^+-channels, by bath application of 4-AP (3–10 mM; Fig. 2d), increased dendritic action-potential amplitude in a concentration-dependent manner (Fig. 3a,e)[10]. Under such conditions, very little amplitude attenuation was observed as action potentials propagated into the dendrites. Single action potentials were transformed into bursts of 2–3 spikes or plateau potentials that led to nearly constant depolarization in the dendrites and continuous repetitive firing in the soma (Fig. 3a,b). Addition of 200 μM $CdCl_2$ or low-Ca^{2+} external solution (0.5 mM Ca^{2+}, 8 mM Mg^{2+}) blocked the generation of plateau potentials and burst firing, indicating that dendritic Ca^{2+} channel activation is required for such activity (Fig. 3a). Upon blockade of transient dendritic K^+ channels, action-potential duration, time to peak, and amplitude were increased, whereas peak rate of rise was not significantly changed (Fig. 3e). These data indicate that blocking dendritic A-type channels may allow dendritic action potentials to continue to depolarize until they reach a peak voltage similar to that of the somatic action-potential. These large-amplitude, back-propagating action potentials activated dendritic Ca^{2+} channels, resulting in a massive influx of Ca^{2+} into the dendrites (Fig. 3a,c). Together our results provide strong evidence that an increased density of A-type K^+ channels in the dendrites of CA1 pyramidal neurons acts to reduce action-potential amplitude and limit the back-propagation of full-amplitude action potentials to only the most proximal dendritic regions. Furthermore, the elevated density of dendritic A-channels does not allow single somatic action potentials to induce

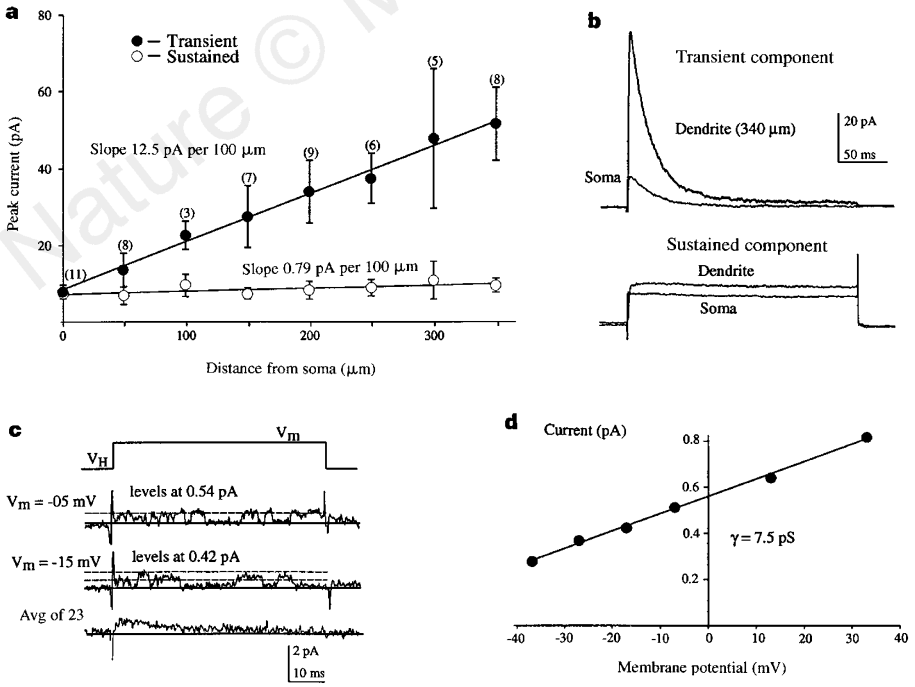

Figure 1 High density of transient K^+ channels in distal dendrites. **a**, The peak outward current amplitude for the transient and sustained components in response to a voltage step from −85 to +55 mV in 11 somatic and 46 dendrite-attached patches (dendrite patches are binned to 50-μm segments). Best fit lines are shown for both components. **b**, Representative traces for both components from the soma and from the dendrites 340 μm from the soma. The two components were separated out from the total outward current by a standard subtraction procedure[14]. **c**, Single-channel recordings of transient A-type channels from cell-attached patches. The patches were voltage-clamped at holding potentials of −65 and −55 mV and stepped to −15 and −5 mV, respectively. Unitary amplitudes are shown. The bottom trace is the ensemble average of 23 sweeps to −15 mV. **d**, *I–V* plot of single transient K^+ channels. Unitary current amplitudes are plotted as a function of membrane potential from four separate experiments (error bars are smaller than the symbols). The mean slope conductance is 7.5 pS.

bursts or repetitive firing, thus maintaining the linear relationship between action-potential firing rate and Ca^{2+} influx[26–29].

The blockade of dendritic A-type channels also allowed action potentials to be initiated in the dendritic compartment (Fig. 3d). In the presence of 4-AP, dendritic current injections or large-amplitude EPSPs could initiate action potentials locally in the dendrites. The effect was likely to be the result of a decrease in dendritic threshold and an increase in the amount of depolarization induced by a given current injection. Although the dendritic membrane was capable of initiating action potentials when A-channel density was reduced, the somatic–axonal region still appeared to have the lowest threshold, because small long-duration dendritic current injections (0.3 nA, 300 ms) evoked axonally initiated action potentials. Thus, A-channel blockade increased the excitability of the dendritic membrane, allowing for the initiation and propagation of fully regenerative action potentials in the dendrites.

The high density of dendritic A-type channels had substantial effects on subthreshold synaptic events propagating through the dendrites. Bath application of 4-AP increased the amplitude, time to peak, and duration of EPSP-shaped voltage transients induced by dendritic current injections (Fig. 4a,b,e). This effect was similar for both somatic and dendritic compartments. Upon wash-in of 4-AP, subthreshold dendritic current injections (~7 mV in soma) were transformed into suprathreshold (>11 mV in soma) bursts of action potentials. In some cases, the action potentials were initiated in the dendritic compartment. As with action-potential shaping, A-channel blockade allowed EPSPs to depolarize further than would occur with a full complement of A-channels present[12,30]. Application of tetrodotoxin (TTX, 300–500 nM) after A-channel blockade revealed that a large fraction of the 4-AP-induced increase in depolarization was due to Na^+ channel activation (Fig. 4c). Thus, A-channels act to counter additional inward current that is induced by subthreshold Na^+ channel activation, effectively eliminating any Na^+ channel EPSP boosting. Although dendritic A-channels reduce the amount of depolarization provided to the soma by synaptic input, the relative amount of voltage decrement occurring from the dendrite to the soma was unchanged (control decrement equalled 52 ± 5% compared with 55 ± 5% with 4-AP) (Figs 4d,e and 5a).

Computer simulations

The whole-cell recordings demonstrate that an increasing density of dendritic A-channels determines action-potential amplitude and threshold, shapes EPSP propagation through the dendrites, and decreases overall membrane excitability. These results show that dendritic Na^+ channel density is sufficient to generate (and even initiate) full-amplitude action potentials once the high A-channel density is reduced. We have used computer simulations to illustrate how this complement of dendritic voltage-gated channels might interact to produce the observed whole-cell properties. Upon constructing a reduced model that contained Na^+ and K^+ channels with the characterized properties, we considered the effect of dendritic voltage-gated channels on the spread of EPSPs towards the soma. The model confirmed that the high density of A-channels may counteract EPSP boosting provided by subthreshold Na^+-channel activation, so that EPSP amplitude is smaller than if the membrane were passive (Fig. 5a). Thus the net effect of the dendritic voltage-gated channels at the estimated densities is to decrease the depolarization provided by the synaptic input. Furthermore, the largest proportion of channel activation, and therefore active current flow, is in the dendritic regions where the synaptic input is located. A proportionally smaller amount of channel activation occurs as the EPSP moves into the more proximal and less depolarized regions, so that they eventually are propagating almost passively. These observations suggest that most EPSP shaping occurs locally at the site of input and helps explain why

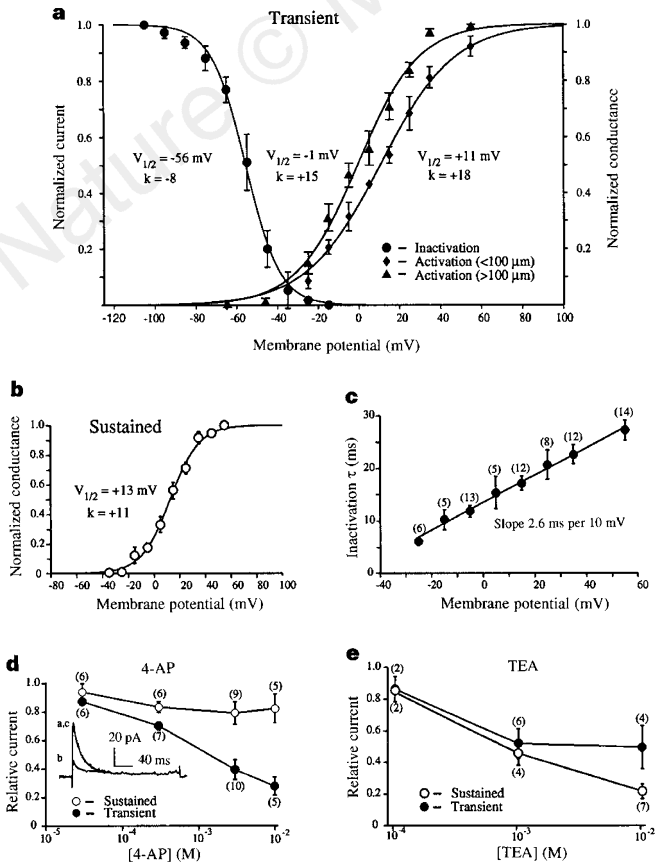

Figure 2 K^+ channel voltage-dependent properties and pharmacology. **a**, Activation and inactivation curves of transient K^+ channels recorded from soma- and dendrite-attached patches. The activation curve for distal dendrites (>100 μm) (triangles) is shifted hyperpolarized compared to that of somatic/proximal dendrites (diamonds) ($V_{1/2} = -1$ and +11 mV, respectively), although their slopes are similar (k is 15 and 18, respectively). The inactivation curve had a $V_{1/2}$ of −56 mV and a k value of −8 (n is 3 to 12). **b**, Activation curve of the sustained component ($V_{1/2} = 13$ mV, $k = 11$, $n = 4$ to 9). **c**, The time constant of inactivation (τ) for the transient channels increases with depolarization. τ is plotted against command potential and fit by a regression line with a slope of 2.6 ms per 10 mV. **d**, Effect of 4-AP on the transient (filled circle) and sustained (open circle) components of the total outward current upon a voltage step from −80 to +40 mV in outside-out patches pulled from the soma and dendrites. 4-AP blocked 50% of the transient current at about 1.4 mM. At no concentration did 4-AP affect more than 20% of the sustained component. Inset: a, trace showing total outward current before application of 4-AP; b, after application of 10 mM 4-AP; c, after washout of 4-AP. **e**, Effect of TEA on the transient (filled circles) and sustained (open circles) components of the total outward current on a voltage step from −80 to +40 mV. TEA at 1 mM blocked about 56% of the sustained current and 50% of the transient current. At 10 mM TEA blocked 80% of the sustained but still only about 50% of the transient current.

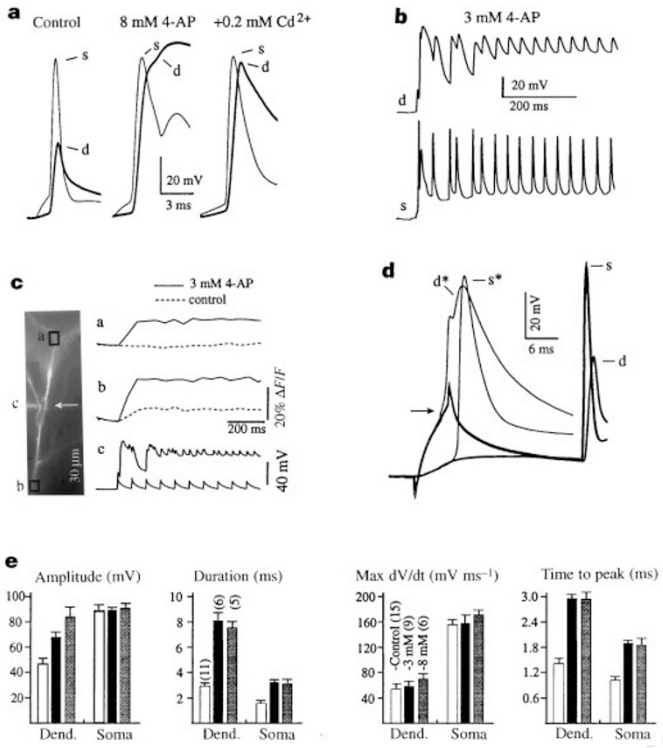

Figure 3 Effect of A-channel blockade on dendritic action potentials. **a**, Under control conditions, current injection into the soma (300 pA, 10 ms) evoked an action potential (somatic recording labelled s) that was severely attenuated upon reaching the dendritic recording pipette (~250 μm, labelled d). Bath application of 8 mM 4-AP caused dendritic action potential amplitude to increase dramatically and a slower plateau potential was also generated. Subsequent addition of 200 μM $CdCl_2$ reduced the duration of the dendritic action potential without affecting the amplitude. **b**, In the presence of normal external Ca^{2+} and 3 mM 4-AP, a single dendritic current injection (1.3 nA, 2 ms) led to prolonged depolarization in the dendrites and repetitive spiking in the soma. Note that the somatic compartment was better able to repolarize than the dendritic compartment. **c**, Fura-2 Ca^{2+} imaging of distal dendrite during a 20 Hz train of back-propagating action potentials. Application of 3 mM 4-AP transformed a moderate and spatially graded influx of Ca^{2+} influx (control; dashed lines) into a large global Ca^{2+} influx (4-AP; solid lines). Traces to the right of the image correspond to the average percentage change in fluorescence ($\Delta F/F$) from the regions inside the appropriately labelled boxes. Bottom trace is dendritic (white arrow) voltage recording for control (smaller action potential) and in 4-AP (plateau) potential). Note that the fidelity of action-potential back-propagation is severely reduced by the generation of a Ca^{2+}-dependent plateau potential during A-channel blockade. **d**, Under control conditions (heavy traces) a 6 ms, 0.9 nA current injection into the dendrite evoked an axonally initiated action potential with a ~15 ms delay. Following 4-AP (8 mM, light traces) wash-in, the same current injection evoked an action potential that was initiated in the dendrite. Arrow points out that apparent threshold was lowered by A-channel blockade. **e**, Plots of action-potential amplitude, duration (at half maximum voltage), maximum rate of rise, and time to peak for control (white bars), 3 mM 4-AP (black bars), and 8 mM 4-AP (grey bars). Number of cells in each group is shown in the maximum rate of rise plot, except for those used for the duration measurements, which are shown separately. The duration measurements include only those neurons that were recorded under conditions of low Ca^{2+} influx (that is, in Cd^{2+} or low Ca^{2+} solutions).

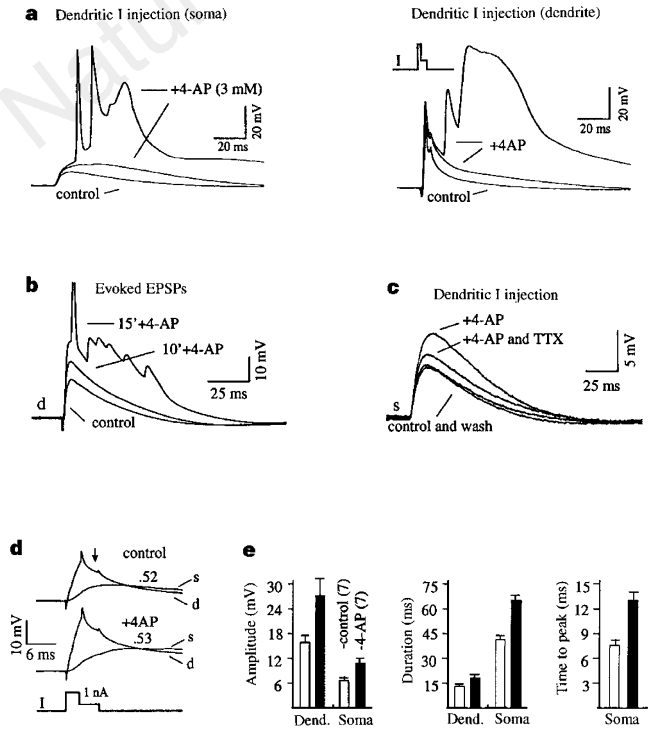

Figure 4 Effect of A-channel blockade on the propagation of EPSPs. **a**, EPSP-shaped voltage transients were produced by a two-step current injection into the dendrite, which under control conditions was subthreshold (~7 mV in the soma). Wash-in of 3 mM 4-AP caused a dramatic increase in the duration and amplitude of the voltage transients in both the somatic (left set of traces) and dendritic (right set of traces) compartments. Upon complete wash-in, the previously sub-threshold current injection evoked a burst of action potentials. **b**, Synaptically evoked EPSPs during control conditions, 10 min and 15 min after perfusion of the dendritic electrode with an internal solution containing 6 mM 4-AP. Previously subthreshold EPSP became suprathreshold evoking bursts of action potentials. Each trace is an average of 5 EPSPs evoked by Schaffer collateral stimulation at 0.25 Hz. **c**, Subthreshold Na^+ channel activation contributes to EPSP amplitude. Bath application of 300 nM TTX subsequent to the application of 3 mM 4-AP, substantially reduced the amount of EPSP amplification induced by A-channel blockade. **d**, The relative amount of EPSP attenuation from dendrite to soma was unchanged by 4-AP application (~50% in both cases). Traces are superimposed dendritic and somatic voltage transients induced by dendritic current injections under control and 4-AP conditions. Note that the amplitude of the dendritic and somatic EPSP increased proportionally with A-channel blockade. Arrow indicates where amplitude measurement was taken from dendritic transient. **e**, Plots of EPSP waveform amplitude, duration (at half maximum voltage), and time to peak for control (white bars) and 3 mM 4-AP (black bars). Number of cells in each group is shown in the amplitude plot.

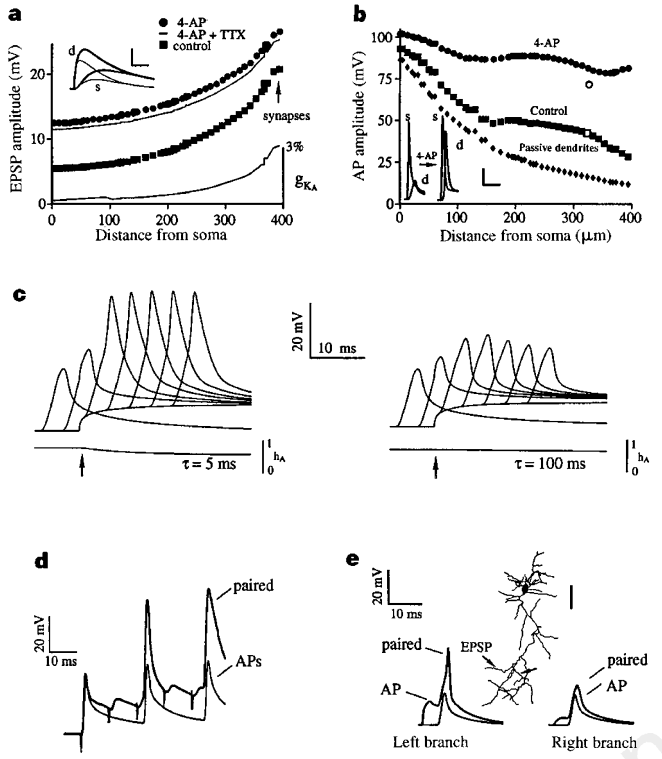

Figure 5 Computer simulations. A-channels shape dendritic EPSPs and action potentials. **a**, A-channels decrease EPSP amplitude primarily at site of input. Peak depolarization of dendrites along path from synaptic input at 390 μm to soma using reconstructed neuron in **e**. Upper plot: normal densities of Na^+ and A-channels (squares), 10% A-channel density (circles) to simulate 4-AP application, and 10% A-channels and no Na^+ channels (solid line) to simulate 4-AP + TTX. Lower plot: peak conductance of A-channels with distance during the EPSP. Note that the conductance decreased rapidly with distance. Inset: waveforms are EPSPs in dendrites (larger pair) and soma (smaller pair) with normal densities (light) and with 10% A-channel density (bold). Scale: 10 mV, 5 ms. **b**, A-channels determine action-potential amplitude. Dendritic action potential amplitude versus distance from soma: normal A-channel density (squares, control), 10% A-channel density (circles, '4-AP'), 10% A-channel density and no dendritic Na^+ channels (diamonds, passive dendrites). Left inset: pairs of somatic (large) and dendritic (small) action-potential waveforms with full A-channel density (left) and 10% A-channel density (right). Decreased A-channel density restricted to a single dendritic branch (open circle) locally increased the amplitude compared to control (open square). Scale: 20 mV, 5 ms. **c**, Inactivation of A-channels increases back-propagating dendritic action-potential amplitude. To inactivate A-channels the dendrite was depolarized (beginning at the arrow) from -67 mV to ~ -55 mV, which decreased the available channel population (h_A) from ~0.8 to ~0.5 with $\tau_h = 5$ ms. Back-propagating action-potential amplitude increased with increasing duration of the preceding depolarization. With the τ_h of inactivation slowed to 100 ms for potentials below -53 mV, (h_A) was decreased only slightly by the depolarization. With increasing duration of preceding depolarization, dendritic action-potential amplitude did not continue to increase. **d**, EPSPs paired with back-propagating action potentials increase dendritic action-potential amplitude. Actual whole-cell recording (not a simulation) from ~240 μm from soma. Action potentials were evoked by 2-ms current injections through a somatic whole-cell electrode at 20-ms intervals. Alone, action-potential amplitude was small (APs). Paired with EPSPs, the action-potential amplitude increased greatly (paired). **e**, Local depolarization selectively increases dendritic action-potential amplitude. Reconstructed pyramidal neurons with symmetrical left and right branches (arrows). Alone, the back-propagating action potential was small and of similar amplitude in both branches (AP). With synaptic input to the left branch (EPSP), the amplitude of the back-propagating action potential increased greatly in the left branch (paired) but not in the right branch (paired). Scale bar, 100 μm.

the relative amount of voltage decrement occurring from the dendrite to the soma is similar with or without dendritic voltage-gated channels.

We next turned to the propagation of action potentials into the dendrites. Previously, the decline of dendritic action-potential amplitude has been attributed to the presence of a density of Na^+ channels that, in everywhere but the axon, is incapable of sustaining a regenerative action potential[31,32]. As shown in Fig. 3, however, A-channel blockade allowed dendritic action potentials to become fully regenerative. In our simulations, incorporation of dendritic A-channels allowed the neuron to produce large-amplitude somatic action potentials that declined as they propagated into the dendrites (Fig. 5b, squares). Decreasing the A-channel density to 10% of its normal value resulted in the action-potential amplitude remaining large throughout the dendritic arbor. Thus, an increasing density of dendritic A-channels determines final action-potential amplitude even when the dendrites contain a uniform Na^+ channel density that can generate fully regenerative action potentials.

We also noted that decreasing the A-channel density in only a single dendritic branch of the model dramatically increased the amplitude of the action potential only in that dendritic compartment (open circle in Fig. 5b). This simulation shows that local modulation of A-channel density can affect membrane excitability in a limited region of the neuron. A-type, K^+-channel activity is controlled by numerous neurotransmitters, chemical messengers, cation concentrations, auxiliary subunits, and by oxidative and phosphorylation states[33–39]. Localized application of such modulatory substances, for example during transmitter release, could lead to a highly local alteration in dendritic membrane excitability. The vast number and diversity of agents that affect these channels may be indicative of their importance in regulating membrane excitability.

A-channel density can also be regulated through membrane depolarization. The voltage-dependent inactivation properties of A-type K^+ channels (Fig. 2) indicate that modest levels of membrane depolarization could decrease the size of the available A-channel population and likewise increase dendritic action-potential amplitude. Such a mechanism would allow subthreshold synaptic activity to regulate dendritic action-potential propagation[13,40]. We used the model to test the hypothesis that moderate dendritic depolarization would significantly inactivate A-type K^+ channels (Fig. 5c) and thus allow dendritic action-potential amplitude to increase. A dendritic compartment was depolarized (arrow in Fig. 5c), and back-propagating action potentials were initiated in the axon before and at progressively later times during the depolarization. During the depolarizations (~12 mV), the fraction of available A-channels (h_A) decreased, and action-potential amplitude increased accordingly. To control for other variables that might influence the amplitude of the action potential, we modified the A-channel model so that inactivation proceeded very slowly ($\tau = 100$ ms) at the steady-state dendritic depolarization, but would inactivate normally when repolarizing the action potential. Thus, during the depolarizing step, the available channels remained essentially constant until the action potential invaded. With these modified A-channels, the amplitude of the action potential increased somewhat with the depolarization (reflecting the increase in Na^+ channel activation), but did not continue to increase throughout the depolarization. Action-potential amplitude decreased later in the depolarization as the Na^+ channels inactivated. Thus, rapid, depolarization-induced inactivation of A-channels is a plausible mechanism for increasing action-potential amplitude in the dendrites.

Under physiological conditions such moderate membrane depolarization can be provided by subthreshold synaptic input. In fact, when back-propagating action potentials are paired with subthreshold synaptic depolarizations, action-potential amplitude (as well as evoked Ca^{2+} influx) is increased in a supralinear fashion[13,41]

(Fig. 5d). One possible explanation for this amplitude boosting is that the depolarization provided by EPSPs inactivates A-channels and decreases their effect on the amplitude of the action potentials. Furthermore, if the local differences in membrane depolarization that occur during synaptic input could similarly affect dendritic excitability, synaptic depolarization might provide a spatially localized amplification of back-propagating action potentials. We simulated this situation by pairing synaptic input onto a single branch of a distal dendrite with back-propagating action potentials. A relatively symmetrical branch point was chosen so that the unpaired action potentials were similar in both daughter branches. When back-propagating action potentials were paired with the localized synaptic input, action-potential amplitude was significantly boosted in the branch receiving synaptic input. As the other branch was only slightly depolarized by the spread of the EPSP, boosting of the action-potential amplitude did not occur. Therefore the susceptibility of A-channels to rapid inactivation during subthreshold synaptic input could provide a mechanism whereby back-propagating action potentials will preferentially invade synaptically active regions of the dendritic arborization. This synaptically regulated propagation of action potentials into specific dendritic branches may play a role in certain forms of hebbian synaptic plasticity[13].

Discussion

The unexpected finding that dendrites of CA1 pyramidal neurons contain a high density of transient, A-type K^+ channels may answer several questions about dendritic function. The presence of these channels could explain why action potentials do not initiate in the dendrites, even during synaptic input, why the amplitude of back-propagating action potentials decreases with distance from the soma, and why there is not a larger boosting of EPSP amplitude, even though inward dendritic conductances are activated. Our results suggest that the linear increase in A-channel density with distance into the dendrites acts, at least transiently, to counter dendritic depolarization. This dampening effect reduces the ability of dendrites to initiate action potentials, decreases the amplitude of back-propagating action potentials, and reduces the magnitude of EPSPs.

Back-propagating action potentials are critical for the induction of associative LTP in CA1 neurons because they allow the output region of the neuron (axon) to communicate with the dendrites[13–15]. Dendritic Na^+ and Ca^{2+} channels provide a mechanism for action potentials to back-propagate into the dendrites. If left unchecked, however, inward conductances in the dendrite result in excessive membrane excitability and unrestricted Ca^{2+} influx (Fig. 3b,c), both of which are detrimental to neuron viability and function. The biophysical characteristics of dendritic A-type K^+ channels make them ideally suited for the task of reducing dendritic excitability. The rapid channel inactivation that occurs at potentials near the resting potential may allow synaptic activity to release local regions of the dendrite from the dampening effect of a high A-channel density. This allows action potentials occurring at the same time as EPSPs to increase in amplitude in a spatially restricted region of the neuron. The inactivation of A-channels by EPSPs and the subsequent amplification of the action potential and evoked Ca^{2+} influx provides a plausible biophysical explanation for the hebbian associativity that is observed in the more distal dendritic regions of these neurons[13].

Finally, the elevated density of dendritic A-channels actually heightens the associativity provided by back-propagating action potentials. Because A-channel density can be modulated by localized synaptic depolarization, full-amplitude action potentials capable of evoking significant Ca^{2+} influx into the more distal dendrites are only generated in synaptically active regions of the dendritic arborization. Alternative models, such as one in which there is a decreasing Na^+ channel density in the dendrites, would not have this feature. Thus, dendritic A-channels provide a dampening effect on dendritic excitability which in turn strengthens the associative link between the input and output regions of the neuron. By shaping action potentials and EPSPs as well as evoked Ca^{2+} influx, A-channels may regulate communication between the soma and dendrites, thereby determining how information is integrated and stored in pyramidal neurons. □

Methods

Hippocampal slices (400 μm) were prepared from 5–8-week-old Sprague–Dawley rats and visualized with a Zeiss Axioskop using infrared video microscopy and differential interference contrast (DIC) optics[5,41]. All neurons had a resting membrane potential between −57 and −72 mV. For all channel recordings, bath solutions contained (in mM): 125 NaCl, 2.5 KCl, 1.25 NaH_2PO_4, 25 $NaHCO_3$, 2.0 $CaCl_2$, 1.0 $MgCl_2$, 25 dextrose and for outside-out patches 1.0 μM TTX (Sigma). The external solution was bubbled with 95% O_2/5% CO_2 at ~22 °C (pH ~7.4) for all recordings. For cell-attached recordings, the pipette solution consisted of (mM): 125 NaCl, 10 HEPES, 2.0 $CaCl_2$, 1.0 $MgCl_2$, 2.5 KCl and 1.0 μM TTX (pH 7.4 with NaOH). For outside-out patch recordings the pipette solution consisted of (mM): 20 KCl, 10 HEPES, 10 EGTA, 120 potassium gluconate, 4.0 Mg_2ATP, 0.3 $Tris_2GTP$, 14 phosphocreatine and 4 NaCl (pH 7.25 with KOH). Pipettes were pulled from borosilicate glass (10–20 MΩ) and coated with sylgard. Tips were visually inspected before use and had uniform diameters of ~1 μm for both dendritic and somatic recordings. Channel recordings, using an Axopatch 1D amplifier (Axon Instruments), were analogue-filtered at 2 kHz and digitally filtered at 1 kHz off-line. Leakage and capacitive currents were digitally subtracted by averaging null traces or scaling traces of smaller amplitude.

For activation plots, chord conductance, calculated from the peak ensemble current amplitude from a holding potential of −85 mV, was normalized to maximum and plotted as a function of test potential. For inactivation, peak ensemble current amplitude for a step to +55 mV was normalized to maximum and plotted as a function of holding potential. Curves are least-square fits of the data to Boltzmann functions. Inactivation time constants were fit by a non-linear, least-squares program and were well fitted by a single exponential. 4-AP, TEA (Sigma) and DTX (Alomone Labs) were added to a solution identical to the bath solution (except for the 10 mM concentrations, in which case dextrose was decreased from 25 to 15 mM) and was applied to the excised patch by a small-bore perfusion pipette. The sustained component often ran down in outside-out patches, therefore only those experiments where a drug washout was obtained were used to construct the dose–response graphs. Error bars represent s.e.m. and the number of patches (n) is given in parentheses.

Whole-cell patch-clamp recordings were made using an Axoclamp 2A (Axon Instruments) and Dagan IX2-700 amplifier in 'bridge' modes. The external recording solution contained (mM): 124 NaCl, 2.5 KCl, 1.2 NaH_2PO_4, 25 $NaHCO_3$, 2.5 $CaCl_2$, 1.5 $MgCl_2$, and 10 dextrose, 0.01 DNQX, bubbled as described at ~35 °C (pH ~7.4). Whole-cell recording pipettes (somatic, 2 to 4 MΩ; dendritic, 7 to 10 MΩ) were pulled from borosilicate glass. The internal solution was the same as above, except that EGTA was omitted. Series resistance for somatic recordings was 6–20 MΩ, whereas that for dendritic recordings was 15–50 MΩ. Dendritic pipettes were coated with sylgard. To measure changes in $[Ca^{2+}]_i$, the fluorescent indicator Fura-2 (20–80 μM) was included in the pipette solution, and a cooled CCD camera (Photometrics) used to record changes in fluorescence[42]. When synaptic stimulation was used, methods were similar to those described[4,42]; DNQX was omitted from the external solution and 10 μM bicuculline was added. Voltages were not corrected for the junction potential (−7 mV) in any of the whole-cell experiments.

Computer simulations were made using NEURON[43] with an integration time-step of 0.025 ms. A biocytin-filled hippocampal pyramidal neuron from an adult male rat was reconstructed using NTS (Eutectics; Fig. 5e). Passive electrical parameters were $R_m = 30,000\ \Omega\,cm^2$, $C_m = 1\ \mu F\,cm^{-2}$ in the somatic compartment and $1.6\ \mu F\,cm^{-2}$ in the dendritic compartments to account for spines. The axial resistivity R_i was 150 Ω cm, except in the axon where R_i was 100 Ω cm.

Synaptic input was modelled as a conductance with dual exponential time course of the form $(1 - e^{-t/\tau_1})e^{-t/\tau_2}$, where $t = 0$ at the onset of the conductance ($\tau_1 = 1.5$ ms and τ_2 was 5–10 ms). Synapses had a reversal potential of 0 mV. EPSPs of 15–20 mV near the site of input were produced by 5–7

simultaneously activated synaptic conductances distributed along ~50 μm of dendrite. Antidromic spikes were evoked by a brief current injection into the most distal axonal segment.

The model included four voltage-gated channels: Na^+, proximal and distal A-type K^+, and DR type. Conductances were set to reproduce the experimentally observed A-type to Na^+ current ratio of ~3 : 1 in cell-attached patches from distal dendrites. We compared the magnitude of the A-type current evoked by a step from −90 to +45 mV to the magnitude of the Na^+ current evoked by a step from −90 to −10 mV to determine this ratio. The DR-type conductance was set to repolarize the action potential in the absence of any A-type current. Conductances in the model were uniformly scaled up by a factor of 2 to yield a somatic action potential with a peak rate of rise of ~200 mV ms^{-1}. The resulting peak conductances were $\bar{g}_{Na} = 0.012$ S cm^{-2}, $\bar{g}_{K_A} = 0.007 + 0.011$ (distance from soma in μm/100) S cm^{-2} and $\bar{g}_{K_{DR}} = 0.0075$ S cm^{-2}. The proximal A-channel model was used within 100 μm from the soma, otherwise the distal model was used. $\bar{g}_{Na}$ and $\bar{g}_{K_{DR}}$ were uniform in the soma and dendrites and increased 10-fold in the axon. Reversal potentials were $E_{Na} = +58$ mV and $E_K = -80$ mV.

Voltage-dependent time constants (τ) and steady-state (ss) values were used to define the instantaneous values of activation (m) and inactivation (h) gates according to: $dx = (x_{ss} - x)(1 - e^{-dt/\tau_x})$, where x is a gate variable, and dx is the change in x made during a time step dt.

The Na^+ channel model was of the form, $\bar{g}_{Na} = 4.2\, m^3 h$, where $m_{ss}(v) = \alpha_m(v))/(\alpha_m(v) + \beta_m(v))$, $\tau_m = 0.8/(\alpha_m(v) + \beta_m(v))$, $\alpha_m(v) = 0.182(v + 25)/(1 - \exp(-(v + 32.5)/4.5))$, and $\beta_m(v) = 0.124(-v - 32.5)/(1 - \exp((v + 32.5)/4.5))$. $h_{ss}(v) = 1/(1 + \exp((v + 58)/5))$. $\tau_h = 1/(\alpha_h(v) + \beta_h(v))$, where $\alpha_h(v) = 0.08(v + 40)/(1 - \exp(-(v + 40)/3))$ and $\beta_h(v) = 0.0005(-v - 10)/(1 - \exp((v + 10)/5))$. The parameters for the Na^+ channel model were derived from refs 5 and 44.

The A-type channel models were of the form $g_{K_A} = m^4 h$. $m_{ss}(v) = \alpha_m(v)/(\alpha_m(v) + \beta_m(v))$, where $\alpha_m(v) = -0.01(v + 21.3)/(\exp((v + 21.3)/-35) - 1)$ and $\beta_m(v) = 0.01(v + 21.3)/(\exp((v + 21.3)/35) - 1)$ for proximal channels. $\alpha_m(v) = -0.01(v + 34.4)/(\exp((v + 34.4)/-21) - 1)$ and $\beta_m(v) = 0.01(v + 34.4)/(\exp((v + 34.4)/21) - 1)$ for distal channels. $h_{ss}(v) = \alpha_h(v)/(\alpha_h(v) + \beta_h(v))$, where $\alpha_h(v) = -0.01(v + 58)/(\exp((v + 58)/-8.2) - 1)$ and $\beta_m(v) = 0.01(v + 58)/(\exp((v + 58)/-8.2) - 1)$ for all A-channels. $\tau_m = 0.2$ ms. $\tau_h(v) = 5 + (2.6$ ms per mV$)(v + 20)/10$ for $v > -20$ mV and 5 ms for $v < -20$ mV.

The DR-type channels were of the form $g_{K_{DR}} = m^4$. $m_{ss}(v) = \alpha_m(v)/(\alpha_m(v) + \beta_m(v))$, where $\alpha_m(v) = -0.0035(v + 30)/(\exp((v + 30)/-13) - 1)$ and $\beta_m(v) = 0.0035(v + 30)/(\exp((v + 30)/13) - 1)$; $\tau_m = 1.8$ ms.

Received 11 November 1996; accepted 30 April 1997.

1. Johnston, D., Magee, J. C., Colbert, C. M. & Christie, B. R. Active properties of neuronal dendrites. *Annu. Rev. Neurosci.* **19,** 165–186 (1996).
2. Yuste, R. & Tank, D. W. Dendritic integration in mammalian neurons, a century after Cajal. *Neuron* **16,** 701–716 (1996).
3. Stuart, G. & Sakmann, B. Active propagation of somatic action potentials into neocortical pyramidal cell dendrites. *Nature* **367,** 69–72 (1994).
4. Magee, J. C. & Johnston, D. Synaptic activation of voltage-gated channels in the dendrites of hippocampal pyramidal neurons. *Science* **268,** 301–304 (1995).
5. Magee, J. C. & Johnston, D. Characterization of single voltage-gated Na^+ and Ca^{2+} channels in apical dendrites of rat CA1 pyramidal neurons. *J. Physiol. (Lond.)* **487,** 67–90 (1995).
6. Schwindt, P. C. & Crill, W. E. Amplification of synaptic current by persistent sodium conductance in apical dendrite of neocortical neurons. *J. Neurophysiol.* **74,** 2220–2224 (1995).
7. Stuart, G. & Sakmann, B. Amplification of EPSPs by axosomatic sodium channels in neocortical pyramidal neurons. *Neuron* **15,** 1065–1076 (1995).
8. Spruston, N., Schiller, Y., Stuart, G. & Sakmann, B. Activity-dependent action potential invasion and calcium influx into hippocampal CA1 dendrites. *Science* **268,** 297–300 (1995).
9. Turner, R. W., Meyers, D. E. R., Richardson, T. L. & Barker, J. L. The site for initiation of action potential discharge over the somatodendritic axis of rat hippocampal CA1 pyramidal neurons. *J. Neurosci.* **11,** 2270–2280 (1991).
10. Andreasen, M. & Lambert, J. D. C. Regenerative properties of pyramidal cell dendrites in area CA1 of the rat hippocampus. *J. Physiol. (Lond.)* **483,** 421–441 (1995).
11. Lipowsky, R., Gillessen, T. & Alzheimer, C. Dendritic Na^+ channels amplify EPSPs in hippocampal CA1 pyramidal cells. *J. Neurophysiol.* **76,** 2181–2191 (1996).
12. Hounsgaard, J. & Midtgaard, J. Intrinsic determinants of firing pattern in purkinje cells of the turtle cerebellum *in vitro*. *J. Physiol. (Lond.)* **402,** 731–749 (1988).
13. Magee, J. C. & Johnston, D. A synaptically-controlled, associative signal for Hebbian plasticity in hippocampal neurons. *Science* **275,** 209–213 (1997).
14. Markram, H. & Tsodyks, M. Redistribution of synaptic efficacy between neocortical pyramidal neurons. *Nature* **382,** 807–810 (1996).
15. Christie, B. R., Magee, J. C. & Johnston, D. The role of dendritic action potentials and Ca^{2+} influx in the induction of homosynaptic long-term depression in hippocampal CA1 pyramidal neurons. *Learn. Mem.* **3,** 160–169 (1996).
16. Klee, R., Ficker, E. & Heinemann, U. Comparison of voltage-dependent potassium currents in rat pyramidal neurons acutely isolated from hippocampal regions CA1 and CA3. *J. Neurophys.* **74,** 1982–1995 (1995).
17. Halliwell, J. V., Othman, I. B., Pelchen-Matthews, A. & Dolly, J. O. Central action of dendrotoxin: Selective reduction of a transient potassium conductance in hippocampus and binding to localized acceptors. *Proc. Natl Acad. Sci. USA* **83,** 493–497 (1986).
18. Storm, J. F. Temporal integration by a slowly inactivating K^+ current in hippocampal neurons. *Nature* **336,** 379–381 (1988).
19. Wu, R.-L. & Barrish, M. E. Two pharmacologically and kinetically distinct transient potassium currents in cultured embryonic mouse hippocampal neurons. *J. Neurosci.* 2235–2246 (1992).
20. Segal, M. & Barker, J. Rat hippocampal neurons in culture: Potassium conductances. *J. Neurophysiol.* **51,** 1409–1433 (1984).
21. Segal, M., Rogawski, M. & Barker, J. A transient potassium conductance regulates the excitability of cultured hippocampal and spinal neurons. *J. Neurosci.* **4,** 604–609 (1984).
22. Solc, C. K., Zagotta, W. N. & Aldrich, R. W. Single-channel and genetic analyses reveal two distinct A-type potassium channels in *Drosophila*. *Science* **236,** 1094–1097 (1987).
23. Sheng, M., Tsaur, M., Jan, Y. N. & Jan, L. Y. Subcellular segregation of two A-type K^+ channel proteins in rat central neurons. *Neuron* **9,** 271–284 (1992).
24. Maletic-Savatic, M., Lenn, N. J. & Trimmer, J. S. Differential spatiotemporal expression of K^+ channel polypeptides in rat hippocampal neurons developing *in situ* and *in vitro*. *J. Neurosci.* **15,** 3840–3851 (1995).
25. Alonso, G. & Widmer, H. Clustering of Kv 4.2 potassium channels in postsynaptic membrane of rat supraoptic neurons: an ultrastructural study. *Neuroscience* **77,** 617–621 (1997).
26. Helmchen, F., Imoto, K. & Sakmann, B. Ca^{2+} buffering and action potential-evoked Ca^{2+} signaling in dendrites of pyramidal neurons. *Biophys. J.* **70,** 1069–1081 (1996).
27. Johnston, D. The calcium code. *Biophys. J.* **70,** 1095 (1996).
28. Callaway, J. C. & Ross, W. N. Frequency dependent propagation of sodium action potentials in dendrites of hippocampal CA1 pyramidal neurons. *J. Neurophysiol.* **74,** 1395–1403 (1995).
29. Jaffe, D. B. *et al.* The spread of Na^+ spikes determines the pattern of dendritic Ca^{2+} entry into hippocampal neurons. *Nature* **374,** 1395–1403 (1995).
30. Nicoll, A., Larkman, A. & Blakemore, C. Modulation of EPSP shape and efficacy by intrinsic membrane conductances in rat neocortical pyramidal neurons *in vitro*. *J. Physiol. (Lond.)* **468,** 693–710 (1993).
31. Rapp, M., Yarom, Y. & Segev, I. Modeling back propagating action potential in weakly excitable dendrites of neocortical pyramidal cells. *Proc. Natl Acad. Sci. USA* **93,** 11985–11990 (1996).
32. Mainen, Z. F., Joerges, J., Huguenard, J. R. & Sejnowski, T. J. A model of spike initiation in neocortical pyramidal neurons. *Neuron* **15,** 1427–1439 (1995).
33. Rudy, B. Diversity and ubiquity of K^+ channels. *Neuroscience* **25,** 729–749 (1988).
34. Gage, P. W. Activation and modulation of neuronal K^+ channels by GABA. *Trends Neurosci.* **15,** 46–51 (1992).
35. Talukder, G. & Harrison, N. L. On the mechanism of modulation of transient outward current in cultured rat hippocampal neurons by di- and trivalent cations. *J. Neurophysiol.* **73,** 73–79 (1995).
36. Chen, Q. X. & Wong, R. K. S. Intracellular Ca^{2+} suppressed a transient potassium current in hippocampal neurons. *J. Neurosci.* **11,** 337–343 (1991).
37. Seridio, P., Kentros, C. & Rudy, B. Identification of molecular components of A-type channels activating at subthreshold potentials. *J. Neurophysiol.* **72,** 1516–1529 (1994).
38. Covarrubias, M., Wei, A., Salkoff, L. & Vyas, T. B. Elimination of rapid potassium channel inactivation by phosphorylation of the inactivation gate. *Neuron* **13,** 1403–1412 (1994).
39. Rettig, J. *et al.* Inactivation properties of voltage-gated K^+ channels altered by presence of β-subunit. *Nature* **369,** 289–294 (1994).
40. Tsubokawa, H. & Ross, W. N. IPSPs modulate spike backpropagation and associated $[Ca^{2+}]_i$ changes in the dendrites of hippocampal CA1 pyramidal neurons. *J. Neurophysiol.* **76,** 2896–2906 (1995).
41. Yuste, R. & Denk, W. Dendritic spines as basic functional units of neuronal integration. *Nature* **375,** 682–684 (1995).
42. Magee, J. C., Avery, R. B., Christie, B. R. & Johnston, D. Dihydropyridine-sensitive, voltage-gated Ca^{2+} channels contribute to the resting intracellular Ca^{2+} concentration of hippocampal CA1 pyramidal neurons. *J. Neurophysiol.* **76,** 3460–3470 (1996).
43. Hines, M. in *Neural Systems: Analysis and Modeling* (ed. Eeckman, F.) 127–136 (Kluwer Academic, Norwell, MA, 1993).
44. Colbert, C. M. & Johnston, D. Axonal action-potential initiation and Na^+ channel densities in the soma and axon initial segment of subicular pyramidal neurons. *J. Neurosci.* **16,** 6676–6686 (1996).

Acknowledgements. We thank P. Pfaffinger and S. Sinha for comments on the manuscript, and R. Gray for help with computer programming and data analysis. This work was supported by grants from the NIMH, NIH, and the Human Frontiers Science Program.

Correspondence and requests for materials should be addressed to D.J. (e-mail: dan@mossy.bcm.Tmc.edu).